



## ORIGINAL ARTICLE

## Adsorption of Copper (II) Ions on a Montmorillonite Clay and its Application as Heterogeneous Catalyst for Knoevenagel Condensation Reaction

Hanane Essebaai<sup>\*1</sup>, Zakaria Benzekri<sup>2</sup>, Houda Serrar<sup>2</sup>, Ahmed Lebki<sup>1</sup>, Said Boukhris<sup>2</sup>, Said Marzak<sup>1</sup>, El Houseine Rifi<sup>1</sup>

<sup>1</sup>Laboratory of Organic Synthesis and Extraction Processes, Department of Chemistry, Faculty of Sciences, Ibn Tofail University, Kénitra, Morocco

<sup>2</sup>Laboratory of Organic, Organometallic and Theoretical Chemistry, Faculty of Science, Ibn Tofail University, Kenitra, Morocco

(Received: 24 October 2020

Accepted: 11 January 2021)

## KEYWORDS

Natural clay;  
Copper;  
Linear method;  
Non-linear method;  
Montmorillonite;  
kinetic model;  
heterogeneous catalyst;  
Knoevenagel reaction

**ABSTRACT:** In the present study, a simplest and most effective method was applied to removal of  $\text{Cu}^{2+}$  ions from an aqueous solution using Montmorillonite clay, nontoxic and abundantly available as an adsorbent. The used adsorbent was characterized using X-ray diffraction (XRD), the X-ray fluorescence spectrometry, Fourier Transform Infrared Spectroscopy (FT-IR) and scanning electron microscope (SEM) coupled with EDX analysis. Adsorption experiments were conducted under various conditions, i.e., contact time, initial concentration, pH of Cu(II) ions solution, adsorbent mass, and particle size. The results proved that the adsorption of Cu(II) ions by Montmorillonite clay was favorable at pH=5.5 with an extraction yield of 85% after 30 min contact. The equilibrium isotherm data were analyzed using the Langmuir and Freundlich equations. In all cases, the adsorption process fitted the second-order kinetics well, and the isotherm equation due to Freundlich showed good fits with the experimental data. In order to value our Cu-Montmorillonite clay (Cu-MC) support, we thought of applying it as recyclable heterogeneous catalyst for the condensation of Knoevenagel. The model reaction was carried out at room temperature, using a quantity of 0.5 mg of catalyst and a volume of 2ml of ethanol, the reaction yield was excellent (87%). The recyclable solid catalyst was effective for five successive cycles, indicating that this clay is a potentially eco-friendly heterogeneous catalyst.

## INTRODUCTION

Montmorillonite Clays actually are excellent adsorbent for the removal of heavy metals from aqueous solutions due to their large specific surface area, chemical and mechanical stability, layered structure and high cation-exchange capacity [1]. They are natural, inexpensive, environmentally friendly and widely available [2-4]. These clays are considered an effective supports in the heterogeneous catalysis presenting several advantages, such as high activity and selectivity [5]. For example,

they were used as excellent catalysts, for, the condensation of Knoevenagel [6], which is one of the most useful reactions and the most used for the formation of carbon-carbon bonds in organic synthesis. Moreover, Knoevenagel condensation products are not just used as intermediates for drug synthesis, polymers, cosmetics and perfumes [7, 8], but also have many uses, including the inhibition of anti-phosphorylation of EGF receptor activity and anti-proliferative [9]. In this present work, the

\*Corresponding author: hanane.essebaai@uit.ac.ma (H. Essebaai)  
DOI: 10.22034/jchr.2021.1913071.1209

focus is on the montmorillonite clay (MC) of Bengurir region due to its importance in the field of adsorption of copper (II) ions and its multi-faceted catalytic application. The adsorption behaviors of  $\text{Cu}^{2+}$  onto montmorillonite clay is evaluated under identical experimental conditions. The adsorption kinetics, effects of pH, adsorbent mass, and adsorption isotherms behavior of copper (II) ions onto MC were investigated. The Cu-Montmorillonite (Cu-MC) catalyst was characterized by scanning electron microscope (SEM) and Fourier Transform Infrared (FTIR), and applied for condensation de Knoevenagel. The distinctive advantages of Cu-

Montmorillonite catalysts with high catalytic activity characteristics will make them a promising group of efficient heterogeneous catalysts.

## MATERIALS AND METHODS

### Material used

In this work, the montmorillonite clay (MC) sample was obtained from the Bengurir area, in the Marrakesh-Safi region in central Morocco. Its exact location is shown in Figure 1 (Jbel Kharrou anticline, a 25 km east of Skhour Rehamna town).

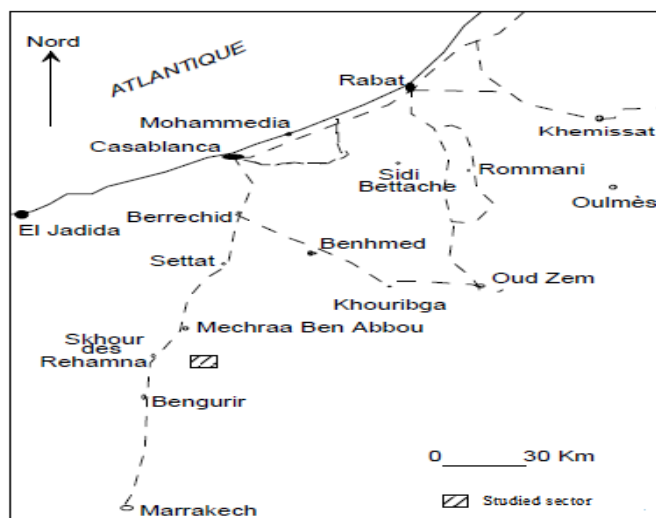


Figure 1. Geological location of the sampling area.

### Characterization of the MC sample

XRD measurements were performed using a XPert PRO Philips diffractometer with  $\text{CuK}\alpha$  radiation ( $\lambda = 1.5406 \text{ \AA}$ ). Clay sample's element composition was defined by X-ray fluorescence spectrometry (Model Axios PW4400, PANalytical) with 1 kW wave-length dispersion. The infrared spectrum was obtained using a BRUKER FT-IR-ATR spectrophotometer, a 0.01g of the clay was diluted with KBr. The spectrum was recorded between  $4000\text{-}400 \text{ cm}^{-1}$ . The morphology and elemental composition of the used clay were done using a scanning electron microscopy (SEM), with an energy dispersive X-ray spectrometer (EDX).

### Adsorption experiment

Adsorption process was applied out at ambient temperature ( $25^\circ\text{C}$ ) by mixed a weighed amount (0.5g) of MC

with 100 mL of  $\text{Cu(II)}$  ions solution at a concentration range from 10 to  $200 \text{ mg L}^{-1}$  were prepared by diluting the stock solution ( $\text{CuSO}_4 \cdot 5\text{H}_2\text{O}$ ). The mixture solutions were agitated at a constant rate for 120 min to reach a full equilibrium state. The influence of pH on  $\text{Cu}^{2+}$  ions adsorption was studied at different initial pH values (adjusted by 0.1M  $\text{H}_2\text{SO}_4$  or 0.1M  $\text{NaOH}$ ) ranging between 3 and 7 using a fixed quantity of adsorbent (0.5g). The remaining copper ion concentration in the supernatant solutions was analyzed by atomic absorption spectrometry (220 AA Spectrometer type).

The adsorbed quantity ( $q_t$ ) by the MC during the adsorptions series and The adsorption percent were determined using the following equations[10]:

$$q_t = (C_i - C_e) \cdot \frac{V}{m}$$

$$\% \text{ Adsorption} = \frac{C_i - C_e}{C_i} * 100$$

With:

$C_i$ : Initial concentration of copper ions ( $\text{mg L}^{-1}$ ).

$C_e$ : Concentration of copper ions at equilibrium ( $\text{mg L}^{-1}$ ).

$m$ : Mass of clay (g).

$V$ : Volume of the solution (mL).

### General procedure for condensation of Knoevenagel:

#### Synthesis of 3a-d compounds

To an equimolar mixture of aromatic aldehyde 1 (1mmol) and malononitrile 2 (1mmol), 0.5mg of our catalytic support (Cu-MC) is added to 2ml of ethanol. The reaction mixture is then agitated at ambient temperature. The progress of the reaction is examined by thin layer chro-

matography (TLC) using the mixture n-hexane/EtOAc (5:1) as eluent. After the completion of the reaction, dichloromethane is then added to the reaction mixture, after that the catalyst is recovered by simple filtration and after that the filtrate is cooled. Then the obtained solid is filtered and recrystallized from ethanol. Compounds 3 a-d are perfectly characterized by IR,  $^1\text{H}$  NMR and  $^{13}\text{C}$  NMR, and confirmed by comparison of their melting points and spectral data with those reported in the literature [11].

## RESULTS AND DISCUSSION

### Characterization of the MC sample

#### X-Ray Diffraction

XRD analysis represented in Figure 2 was used to investigate the structure of the MC.

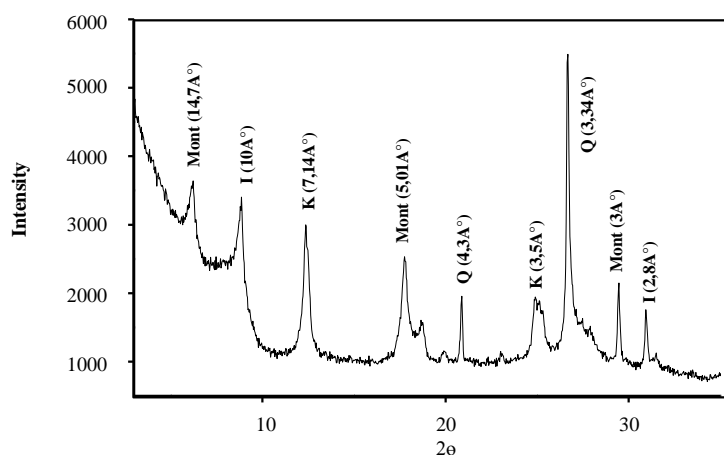


**Figure 2.** X-ray diffraction spectra of the MC.  
(Mont: montmorillonite, K: Kaolinite, Q: Quartz, I: Illite)

The X-Ray Diffraction analysis indicated that the mineralogical composition of the used clay sample contains Montmorillonite as the major clay mineral associated with a mixture of Illite, Quartz, and Kaolinite.

#### X-ray fluorescence analysis

The composition of the MC was characterized by X-ray fluorescence analysis, and results are represented in

Table 1. XRF results in this Table show that silica, calcium, iron, alumina, and magnesium oxides are the main constituents of the used clay. As confirmed by XRD analysis, the predominant content of  $\text{SiO}_2$  is due to the presence of Quartz. On the other hand, the presence of a higher content of  $\text{MgO}$  and  $\text{CaO}$  suggests that  $\text{Mg}^{2+}$  and  $\text{Ca}^{2+}$  are the predominant exchangeable cations. The higher content of  $\text{K}_2\text{O}$  is explained by the presence of Illite [12].

**Table 1.** Chemical composition of the MC.

Composition	Content (%)
SiO <sub>2</sub>	51
Al <sub>2</sub> O <sub>3</sub>	21.7
Fe <sub>2</sub> O <sub>3</sub>	3.91
CaO	3.16
K <sub>2</sub> O	3.15
MgO	3.12
Na <sub>2</sub> O	1.28
TiO <sub>2</sub>	0.66
P.A.F	11.2

**Infrared spectroscopy**

Characteristic infrared absorption bands of the investigated clay were determined by FTIR spectra. As shown in Figure 3, the band located at 3600 cm<sup>-1</sup> is attributed to the stretching vibration of clay hydroxyl group O-H, while those located at wavenumbers of 1428 cm<sup>-1</sup> and 1634 cm<sup>-1</sup> are associated with stretching vibrations of the H<sub>2</sub>O intercalated in the MC. The characteristic peaks occur-

ring around 1000 cm<sup>-1</sup> and 519 cm<sup>-1</sup> can be assigned to Si-O and Al-O-Si bending vibration, respectively. It observed from the infrared spectrum that the obtained results confirm the presence of the siliceous compounds, which is in agreement with the results obtained from the X-ray diffraction and based on the bibliographic data [13-15].

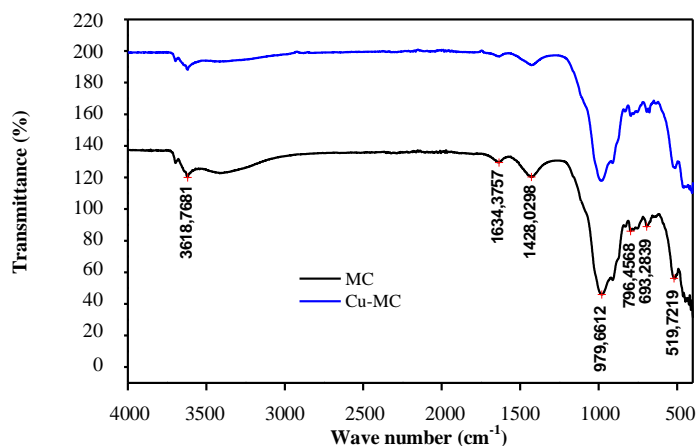


**Figure 3.** IR spectra of MC.

It is noted that after the adsorption of copper ions the band observed around 976,66 cm<sup>-1</sup> is due to the asym-

metric valence vibration of Si-O band moved to 982,55 cm<sup>-1</sup> due to the adsorption of copper (Table 2).

**Table 2.** Assignment of vibration bands before and after adsorption.

Natural clay (MC)	Clay after extraction (Cu-MC)	Functions
3618.7	3618.7	-OH
1634.3	1634.3	O-H
1428.02	1427.06	O-H
976.66	982.55	Si-O
796.45	795.49	Si-O du quartz
693.28	676.8	M-O
519.72	518.75	O-Si-O and Si-O-Si

The comparison of the spectra before and after copper (II) adsorption shows that vibrations of O-H and Si-O bonds are sensitive to the adsorption reaction. In fact, a notable shift in their vibrational wave numbers is observed indicating a change in the vibrational energy of the functional group. These results approve the involvement of these groups in the binding of Cu (II) to MC [16]. The replacement of the vibration band of the O-H bond towards low wave numbers after adsorption implies a decrease in the force constant and a reduction in the covalent character of this bond. As regards the Si-O bond the opposite phenomenon is observed. In fact, the number of valence vibrations of this bond increased after adsorption indicating an increase in covalent character.

**Scanning electron microscope**

Surface morphology and elemental composition of the investigated clay before and after copper adsorption were analyzed using SEM-EDX. Figure 4 shows the morphology and composition of the MC and Cu-MC. Before the adsorption, results indicate the existence of particles with irregular appearance and different sizes mainly because of its crystallinity. After copper adsorption, MC morphology seems a bit homogeneous and somewhat with less open porosity.

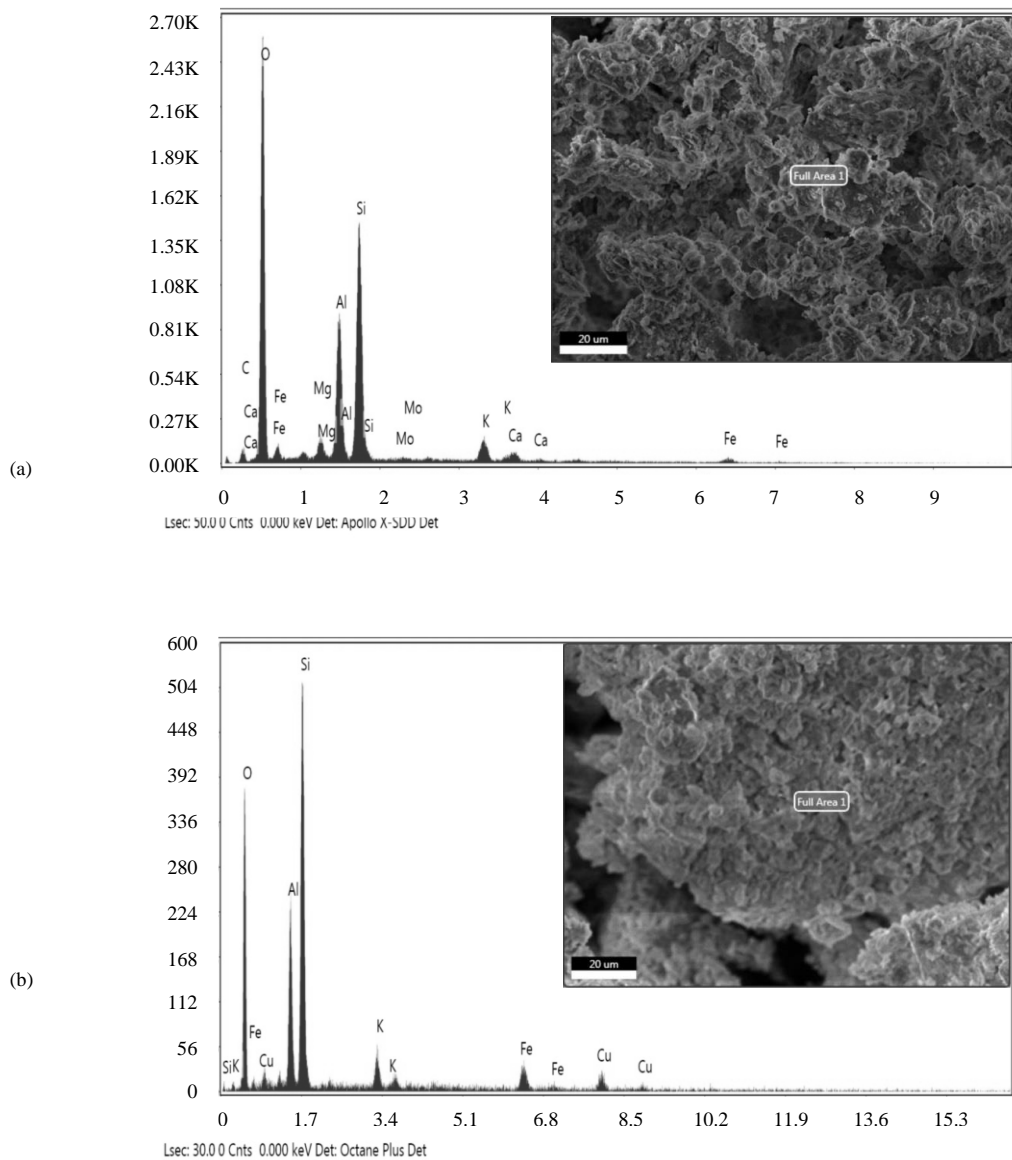


**Figure 4.** Scanning electron micrographs and EDX spectrograms of MC and Cu-MC.

The analysis spectra of these two samples clay show from the shape and intensity of the revealed peaks that silicon and oxygen are the main elements of clay. It is also recorded that the aluminum intensity is relatively important compared to the other elements of clay. The EDX spectrum of the MC (Figure 4a) demonstrate the absence of the characteristic peak of copper. On the other hand, the clay spectrum after adsorption indicates the appearance of copper peaks. This means that the copper is inserted in the MC, which explains the compacted MC surface morphology that detected after Cu (II) ion adsorption (Figure 4b). This result illustrates that Cu (II) ion adsorbed on the

MC surface.

#### Adsorption characteristics of $\text{Cu}^{2+}$ on natural clay

##### Effect of contact time

The adsorption capabilities of the Cu (II) ions on the MC was evaluated at different concentrations and adsorption times. Experiments were conducted at a copper concentration range from 10 to 200mg L<sup>-1</sup> and a time interval of 120minutes. Results of this analysis are represented in Figure 5.

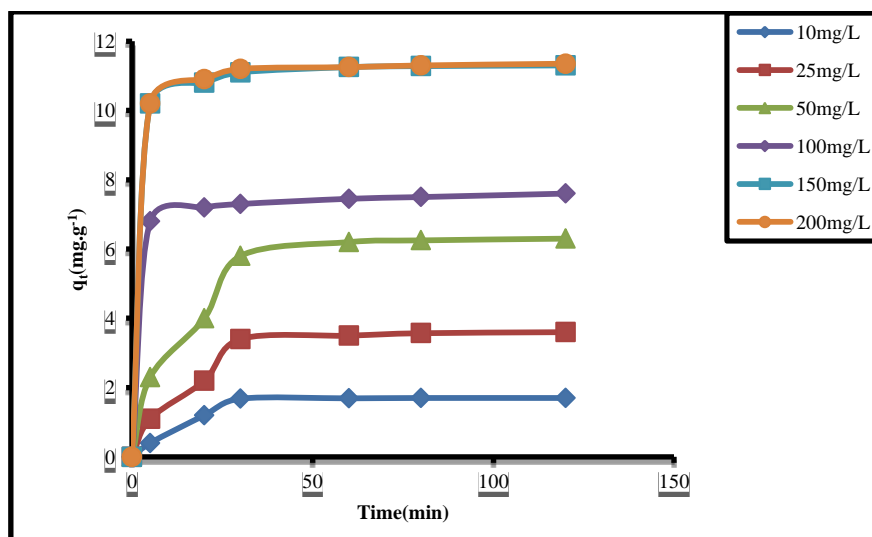


Figure 5. Effect of contact time on  $\text{Cu}^{2+}$  adsorption onto MC at different initial concentration. ( $V_{\text{aq}} = 100\text{ml}$ ,  $\text{pH}=5.5$ ,  $m_{\text{clay}}=0.5\text{g}$ ,  $T=25^\circ\text{C}$ ).

The data presented that the adsorption of  $\text{Cu}^{2+}$  ions on MC was fast and the equilibrium was reached after 30min for a lower  $\text{Cu}^{2+}$  concentration (10 mg L<sup>-1</sup>) while it reaches after 40min for higher concentrations (25 to 200mg L<sup>-1</sup>) (Figure 5). The adsorption process is fast at the beginning of the reaction due to the abundant adsorption sites in the clay surface, and then it becomes constant due to saturation. Similar adsorption behavior was observed by other researchers [10].

##### Effect of pH

Solution pH is the best variable the adsorption of Cu(II) ions. To study pH influence, experiments were conducted

at 3-7 pH range with 10mg L<sup>-1</sup> of  $\text{Cu}^{2+}$  ions. By analyzing results in Figure 6; we could see that the adsorbed quantity of Cu (II) on the MC increases with increasing solution pH. At high acidic solutions ( $\text{pH}<4$ ), Cu (II) adsorption rate is very low. The decreased adsorption rate at this pH is associated to the existence of higher amount of  $\text{H}^+$  ions, which could occupy a large number of adsorption sites, causing a decrease in  $\text{Cu}^{2+}$  adsorption [17]. When pH increases ( $\text{pH} \geq 4$ ), the adsorption rate increases due to the decrease in  $\text{H}^+$  cations [18].

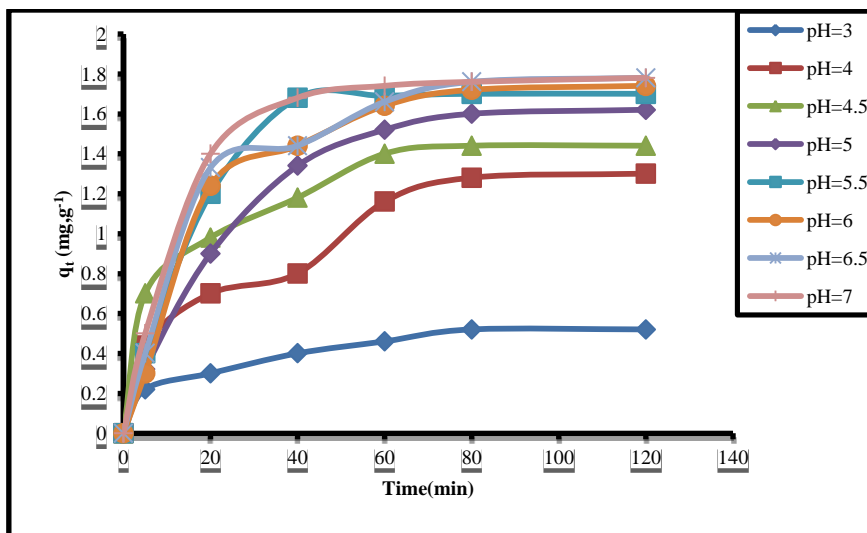


**Figure 6.** Effect of pH on the adsorption capacity of  $\text{Cu}^{2+}$ . ( $V_{\text{aq}} = 100\text{ml}$ ,  $[\text{Cu}^{2+}]_i = 10\text{mg.L}^{-1}$ ,  $m_{\text{clay}} = 0.5\text{g}$ ,  $T = 25^\circ\text{C}$ ).

### Effect of mass

The purpose in this study is to specify the amount of the MC powder needed to eliminate the maximum amount of copper (II) ions optimizing the mass of material is of significance to boost the cost-effectiveness in any treatment process [19]. The clay mass effect was studied on

$\text{Cu}^{2+}$  ions elimination from aqueous solutions by varying the quantity of MC from 0.1 to 2g while keeping other parameters constant. The results of this study are illustrated in Figure 7.

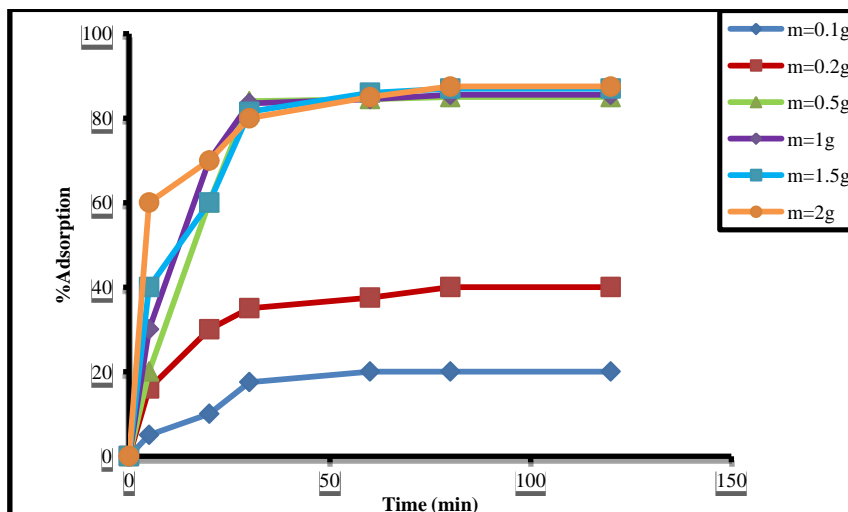


**Figure 7.** Effect of agitation time and clay mass on the percent adsorption. ( $V_{\text{aq}} = 100\text{ml}$ ,  $[\text{Cu}^{2+}]_i = 10\text{mg L}^{-1}$ ,  $\text{pH} = 5.5$ ,  $T = 25^\circ\text{C}$ ).

The % adsorption increases from 19 to 88 with increasing adsorbent mass because of the availability of adsorption sites [20] therefore in order to achieve maximum removal efficiency, a 0.5g was selected as the optimal mass.

### Effect of particle size

To study the influence of MC particles size on the  $\text{Cu}(\text{II})$  ions adsorption capacity, experiments were performed using initial solutions, containing 100ml copper(II) solution at a concentration of  $10\text{mg L}^{-1}$  and 0.5g MC at different particles size ( $D \leq 0.63\text{mm}$ ,  $D \leq 0.32\text{mm}$ ,  $D \leq 0.225\text{mm}$  and  $D \leq 0.112\text{mm}$ ).

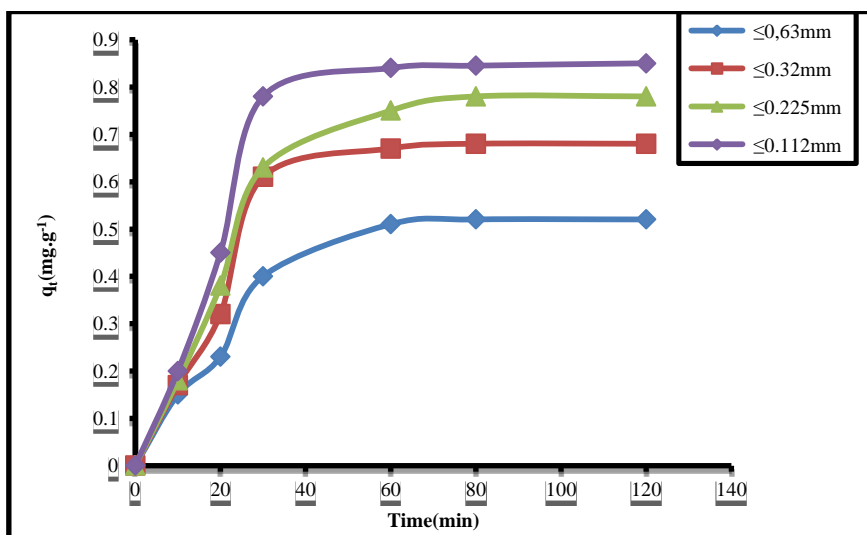


**Figure 8.** Effect of particle size on the Cu (II) adsorption onto MC. ( $V_{aq} = 100\text{ml}$ ,  $[Cu^{2+}]_i = 10\text{mg L}^{-1}$ ,  $pH_i=5.5$ ,  $m_{clay}=0.5\text{g}$ ,  $T=25^\circ\text{C}$ ).

It is clear that decreasing the clay particle size from 0.63 to 0.112 mm has increased the adsorption of Cu (II) ions and hence increased the maximum adsorption capacity. This improvement in adsorption is because of increasing the total surface area of MC particles, and as a result, more active sites are exposed to Cu (II) ions [21].

To explain this phenomenon it may be necessary to discover the total surface area of each size of clay particles by the titration method using blue methylene. Table 3 shows the variation of the total surface area with the size of MC particles.

**Table 3.** Particle size and total Surface Areas of MC.

Particle size (mm)	D≤0.63	D≤0.32	D≤0.225	D≤0.112
R (%)	52	68	78	85
Total specific area (m <sup>2</sup> .g <sup>-1</sup> )	134	138	142	145.23

The small particles of MC have a much larger surface area than the larger MC particles. This large surface area allows the clay to hold a greater quantity of Cu (II) ions.

**Kinetic study**

**Pseudo-first-order (PFO) and Pseudo-second-order (PSO) models**

The PFO equation was proposed by Lagergren [22] in 1898. It has the next differential form:

$$\frac{dq}{dt} = k_1(q_e - q)$$

Its linearized form is:

$$\ln(q_e - q_t) = \ln(q_e) - k_1 t$$

Where:

$q_t$ : Quantity of Cu(II) ions adsorbed at time t (mg g<sup>-1</sup>)

$q_e$ : Quantity of Cu(II) ions adsorbed at equilibrium time (mg g<sup>-1</sup>)

$k_1$ : Rate constant (1 min<sup>-1</sup>).

The PSO model assumes that the uptake rate is second order with respect to the available surface sites [23]. It has the following differential form:

$$\frac{dq}{dt} = K_2(q_e - q)^2$$

Its linearized form is:

$$\frac{t}{q_t} = \frac{1}{k_2 q_e^2} + \frac{1}{q_e} t$$

With,

$k_2$  : Rate constant ( $\text{g} (\text{mg min})^{-1}$ ).

Figures 9 and 10. The kinetics parameters are listed in Table 4.

The adsorption kinetics of  $\text{Cu}^{2+}$  on MC presented in

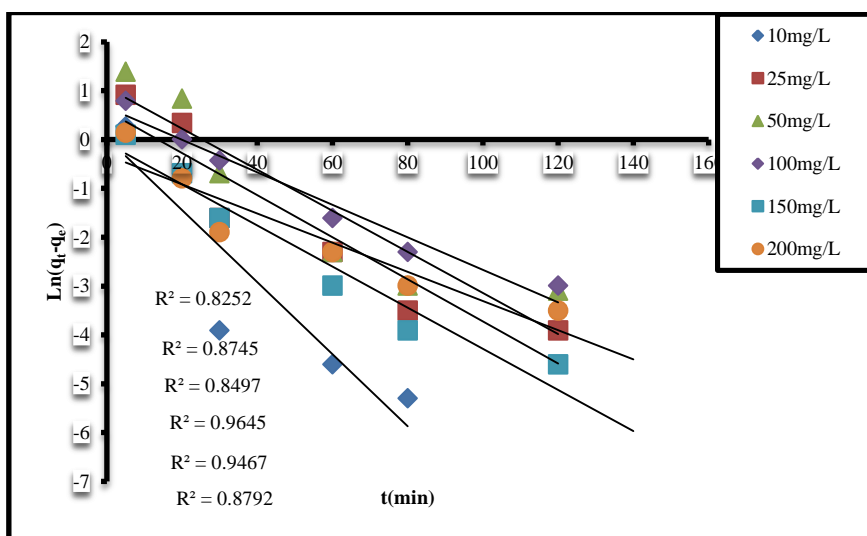


Figure 9. Plot of pseudo-first-order kinetics for various initial concentrations.

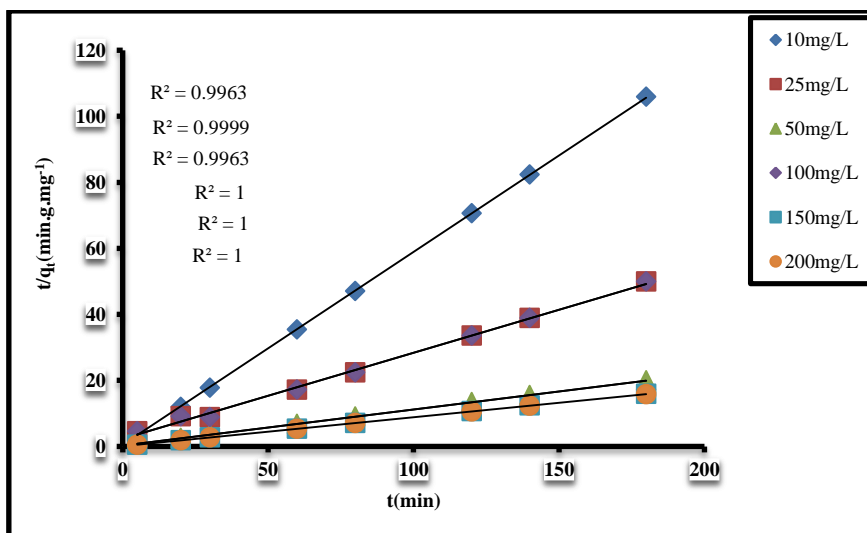


Figure 10. Plot of pseudo-second-order kinetics for various initial concentrations.

As we can see from Table 4, the coefficients of determination  $R^2$  for the kinetic model of pseudo-first-order (PFO) and are lower than those of the pseudo-second-order (PSO).

These obtained results show that the pseudo-second-order kinetic model is better described for the  $\text{Cu}(\text{II})$  adsorption on natural clay [24-26]. In addition, the theoretical ( $q_{e,cal}$ ) values calculated by the pseudo-second-order model are very close to the experimental adsorption values ( $q_{e,exp}$ ) for all concentrations.

**Intraparticle Diffusion model (IPD).**

The diffusion mechanism was further examined by the equation of the IPD rate, expressed in equation [27]:

$$q_t = k_d t^{1/2} + C$$

Where :

$K_d$ : Rate constant ( $\text{mg g} \cdot \text{min}^{-1}$ ).

C: Intercept at the origin.

The  $K_d$  was retained from the slope of the  $q_t$  curve with respect to  $t^{1/2}$ . The applying of this model to the experimental findings is manifest in Figure 11, and the values of the determinants are stated in the Table 4. As designated the presence of the intercept  $C \neq 0$  shows that the traces do not pass through the origin. The attendance of the boundary layer effect (C) showed that there's a adsorption

of Cu(II) ions on the MC surface indicating that the inner diffusion is not the only rate limiting step of adsorption.

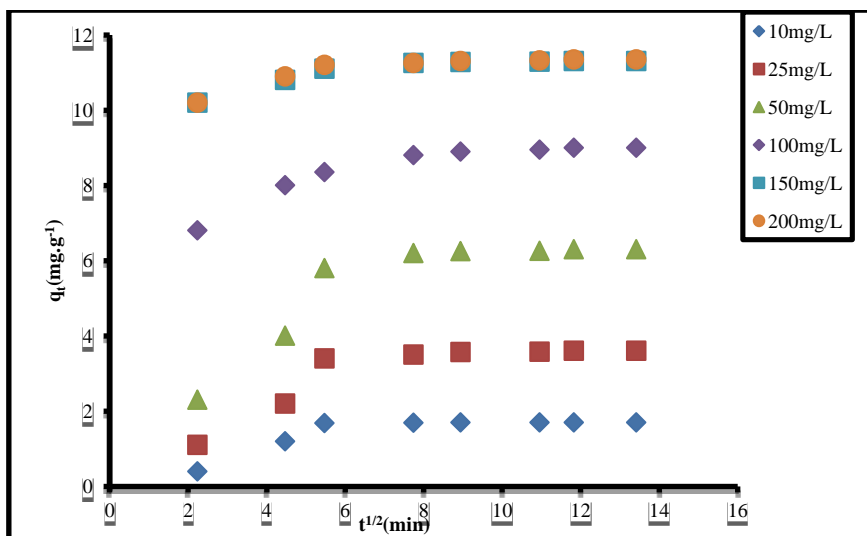


Figure 11. Plot of Intraparticle diffusion model for various initial concentrations of Cu(II)

Table 4. Parameters of adsorption kinetic models.

[Cu <sup>2+</sup> ] (mgL <sup>-1</sup> )	Pseudo-first ordre			pseudo-second ordre			Intra-particle Diffusion		
	k <sub>1</sub>	q <sub>e</sub>	R <sup>2</sup>	k <sub>2</sub>	q <sub>e</sub>	R <sup>2</sup>	K <sub>d</sub>	C	R <sup>2</sup>
10	0.073	1.028	0.825	0.172	1.711	0.999	0.112	0.419	0.568
25	0.047	1.791	0.874	0.160	3.837	0.996	0.258	0.856	0.654
50	0.042	2.891	0.849	0.026	6.650	0.997	0.440	1.636	0.676
100	0.033	1.921	0.964	0.003	9.12	1	0.483	4.036	0.765
150	0.042	0.925	0.946	0.0004	11.360	1	0.540	5.928	0.661
200	0.029	0.721	0.879	0.0004	11.393	1	0.541	5.957	0.661

**Isotherm Study**

Adsorption isotherms are developed to correlate adsorption equilibrium for the adsorbent materials characterization and also for the design of the industrial adsorption metals process.

In this research work, two isotherms models have been established (Langmuir, Freundlich) to determine the experimental data of the adsorption procedure. These isotherms are broadly used isotherms by researchers [28].

The linear and non-linear regression method was performed to detect the best isotherm. Linear and non-linear equations are presented in Table 5. [29]. The Langmuir and Freundlich isotherms models can be designated into linear and one non-linear forms as assumed in Table 5. Where K<sub>L</sub> and K<sub>F</sub> signify Langmuir and Freundlich constants respectively [30].

Table .5. Adsorption isotherm equations.

Isotherms	Equations	linear forms	Plot.
Lang-1		$\frac{C_e}{q_e} = \frac{1}{K_L \cdot q_{max}} + \frac{C_e}{q_{max}}$	$\frac{C_e}{q_e} = f(C_e)$
Lang-2		$\frac{1}{q_e} = \left(\frac{1}{K_L \cdot q_{max}}\right) \frac{1}{C_e} + \frac{1}{q_{max}}$	$\frac{1}{q_e} = f\left(\frac{1}{C_e}\right)$
Lang-3	$q_e = \frac{q_m K_L C_e}{1 + K_L C_e}$	$\frac{q_e}{C_e} = K_L \cdot q_{max} - K_L \cdot q_e$	$\frac{q_e}{C_e} = f(q_e)$
Lang-4		$q_e = q_{max} - \frac{1}{K_L} \frac{q_e}{C_e}$	$q_e = f\left(\frac{q_e}{C_e}\right)$
Freundlich	$q_e = K_F C_e^{1/n}$	$Lnq_e = \frac{1}{n} LnC_e + LnK_F$	$Lnq_e = f(LnC_e)$

Four different error deviations ( $x^2$ , ARE, EABS, and HYBRID) were tested to evaluate the applicability of each model isotherm equation to the experimental data (Table 6) using the solver add-in functions of Microsoft Excel software

Table 6. Equations of error deviations.

Error functions.	Equations.	Ref.
Determination coefficient ( $R^2$ )	$R^2 = \frac{\sum(q_{max} - \bar{q}_e)^2}{\sum(q_{max} - \bar{q}_e)^2 + \sum(q_{max} - q_e)^2}$	[31]
Chi Square Statistic ( $x^2$ )	$x^2 = \sum \frac{(q_{e,cal} - q_{e,exp})^2}{q_{e,exp}}$	[29]
Average relative error (ARE)	$\frac{100}{n} \sum_{i=1}^n \left  \frac{q_{e,exp} - q_{e,cal}}{q_{e,exp}} \right $	[32]
Sum of the absolute errors (EABS)	$\sum_{i=1}^n  q_{e,exp} - q_{e,cal} $	[33]
Hybrid fractional error function (HYBRID)	$\frac{100}{n-p} \sum_{i=1}^n \frac{(q_{e,exp} - q_{e,cal})^2}{q_{e,exp}}$	[34]

**Linear isotherm models**

To describe the relationship between the adsorption capacity  $q_e$  and its equilibrium concentration  $C_e$ , Four linear forms of Langmuir isotherm Figure12, and Freundlich isotherm Figure13 were studied. The adsorption intensity for adsorbent used in this study found from the linear Freundlich isotherm model is higher ( $n > 1$ ) imply-

ing a good adsorption process with lower errors functions and higher  $r^2$  value. For linear Langmuir isotherm  $x^2$ , ARE, EABS, and HYBRID were higher than Freundlich isotherm. Hence, Freundlich model is the befitting isotherm to study the elimination of Cu (II) ions on used clay surface [33].

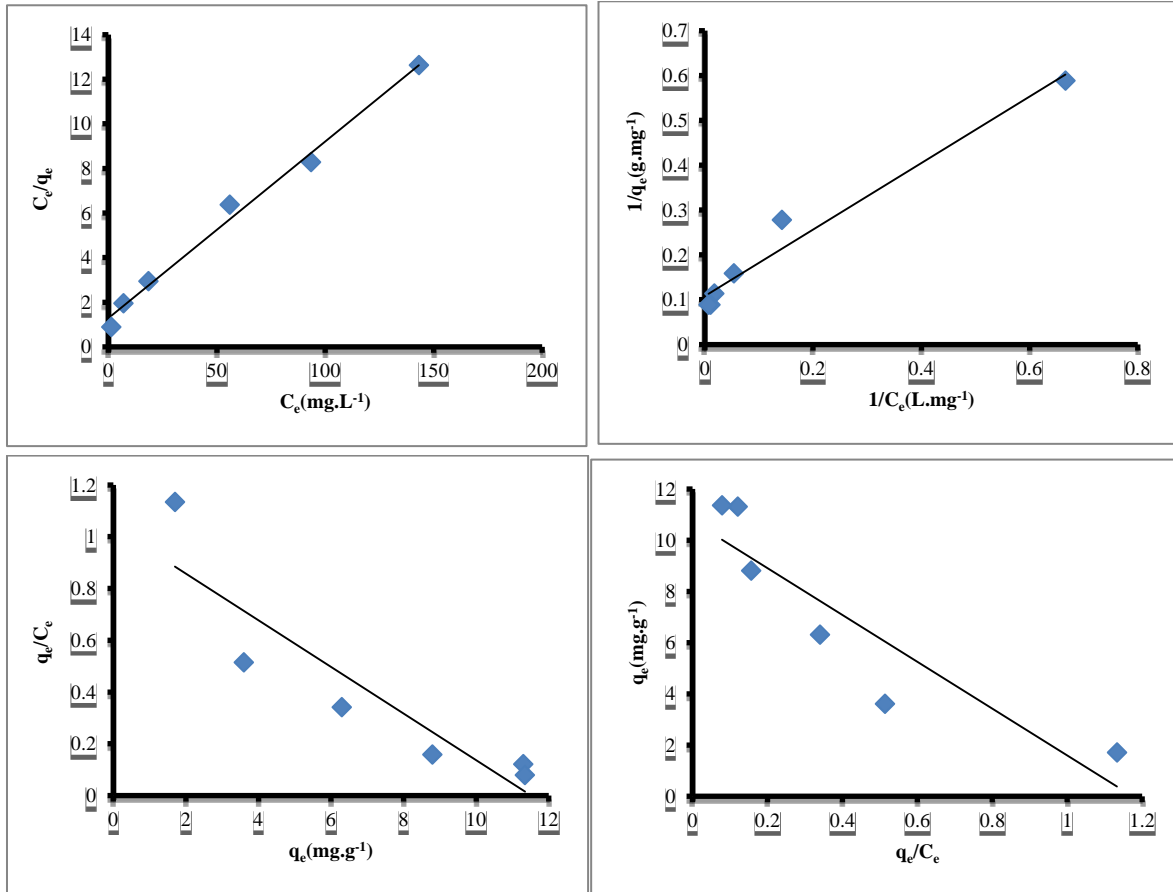


Figure12. Lang-1; Lang-2; Lan-3; Lang-4 linear isotherms.

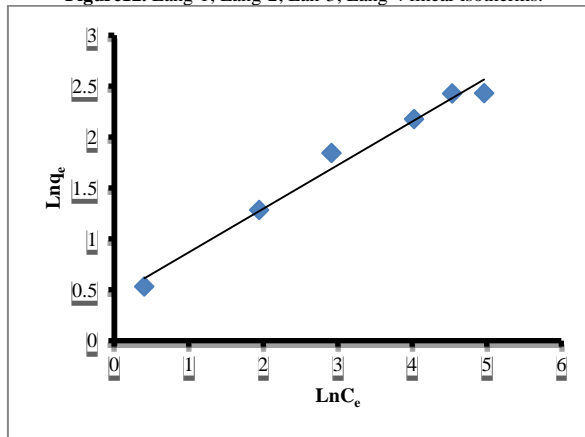


Figure13. Freundlich linear isotherm.

Table 7. Linear isotherm parameters for adsorption of Cu (II) ions on MC.

Isotherms	Lang-1	Lang-2	Lang-3	Lang-4	Freundlich
	$q_m=12.42$	$q_m=9.241$	$q_m=11.5164$	$q_m=10.902$	$1/n=0.4282$
Isotherms parameters	$K_L=0.0719$	$K_L=0.146$	$K_L=0.09$	$K_L=0.107$	$K_F= 1.553$
$R^2$	0.99	0.96	0.82	0.82	0.98
$r^2$	<b>0.99</b>	0.98	0.91	0.90	<b>0.99</b>
$X^2$	4.57	1.5921	19.6534	3.38	<b>0.40</b>
ARE	31.78	71.69	1.43	6.13	16.85
EABS	10.02	4.30	6.21	10.37	9.06
HYBRID	114.43	39.80	84.6	491.33	54.40

**Non-linear isotherm models.**

Non-linear method is used to detect the non-linear forms of Langmuir and Freundlich isotherm as presented in Figures 14 and 15. As observed from Table 8, the two

isotherms had the same value of  $r^2 = 0.99$  but the Freundlich isotherm had the lowest error functions. So Freundlich isotherm is the best-fitting isotherm.

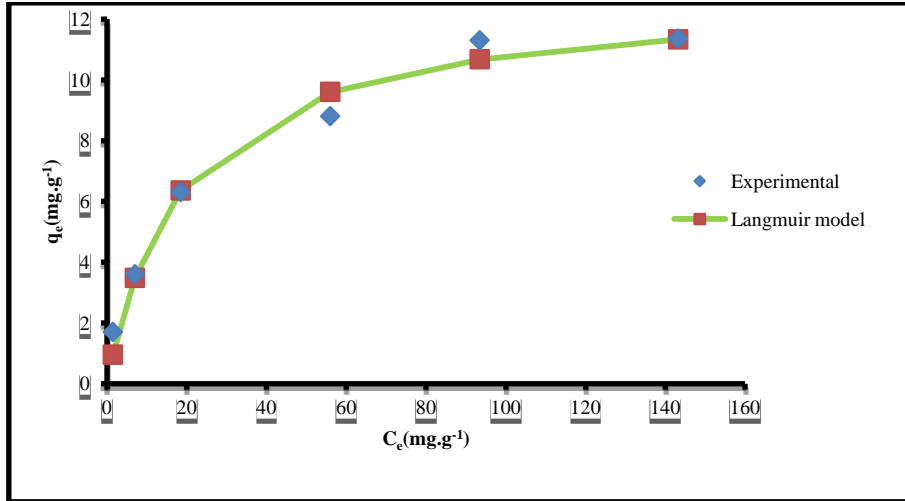


**Figure 14.** Non-Linear fitting of the Langmuir isotherms models.

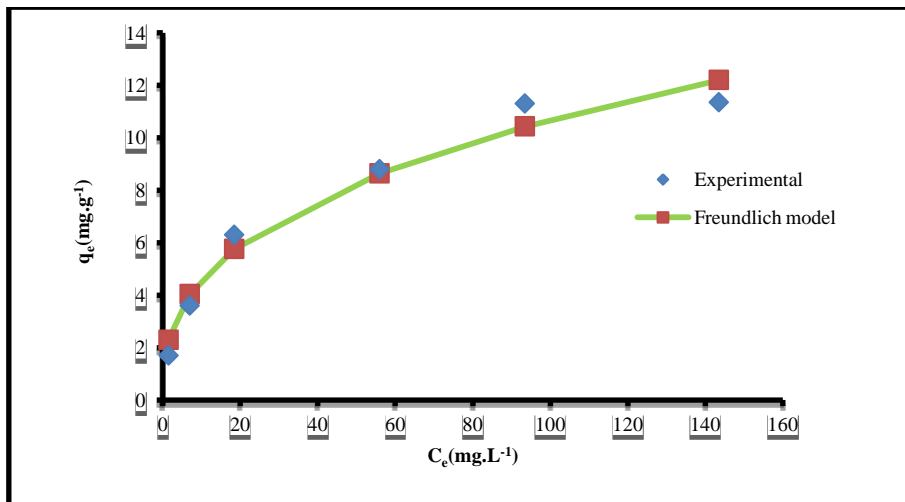


**Figure 15.** Non-Linear fitting of the Freundlich isotherms models.

**Table 8.** Non-linear isotherm parameters for adsorption of Cu (II) ions on MC.

Isotherms	Langmuir	Freundlich
Isotherms parameters	$q_{max}=12.819$	$1/n=0.3634$
	$K_L=0.05$	$K_F= 1.97$
<b>R<sup>2</sup></b>	0,728	<b>0,938</b>
<b>r<sup>2</sup></b>	<b>0.99</b>	<b>0.99</b>
<b>X<sup>2</sup></b>	0.444	<b>0.440</b>
<b>ARE</b>	11.04	<b>5.28</b>
<b>EABS</b>	0.66	<b>0.31</b>
<b>HYBRID</b>	11.12	11.00

### Comparison of linear and non-linear isotherm.

As stated in Table 7 and Table 8 the linear forms had the lowest  $r^2$  value than the non-linear forms.

Thus, the different results for four linear forms of Langmuir isotherm are because the error structure will get various upon linearizing the nonlinear equation. The error deviations may vary depending on the way the equation is linearized. Various results for the four linearized equations are also due to the different axial settings, that would amend the result of linear regression and influence the determination process [35]. So, it will be more suitable to use non-linear method to estimate the parameters involved in the isotherm. Also, non-linear method had an advantage that the error deviations do not get altered as in linear technique. Hence the non-linear method is an important method to get the isotherm parameters.

### Application of studied clay as a catalyst for condensation of Knoevenagel.

Catalytic test for Knoevenagel condensation reaction.

Initially, we searched to develop a simple and efficient process for Knoevenagel condensation. First, we carried out of 4-chlorobenzaldehyde (1a) with malononitrile (2) in the presence of 3 mg of our catalytic support in 2 ml of ethanol at room temperature. This reaction is considered as a model reaction (Figure16). Based on the obtained

results, It is noted that in the absence of the catalyst, the product 3a is obtained for after 180 minutes with a low yield of 54% (Table 9, Entry 1). On the other hand, the same reaction carried out in the presence of one of our catalysts leads to the desired product 3a with a yield of 72% and 87% respectively (Table 9, Entry 2-3). The clay after adsorption (Cu-MC) is the adequate catalyst for this transformation in terms of time and yield (Table 9, Entry3). After determining the right, catalyst for this reaction, then we performed the model reaction in 2 ml of different solvents in the presence of 3 mg of our catalytic support at room temperature. According to Table 10, ethanol is the best solvent for this transformation in terms of time and efficiency of the reaction (Entry1). To estimate the optimal amount of our catalyst needed to condense 4-chlorobenzaldehyde with malononitrile in 2 ml of ethanol at room temperature, we varied the catalyst mass from 0.5 to 5mg In terms of yield, we noted that 0.5 mg of the catalyst gave the best result (Table 11, Entry 1). When the used mass exceeds the optimal amount of the catalyst, we observe a slight decrease in the yield (Table 11, Entry 2-6). This can be explained by the dispersion of the substrates on the surface of the support.

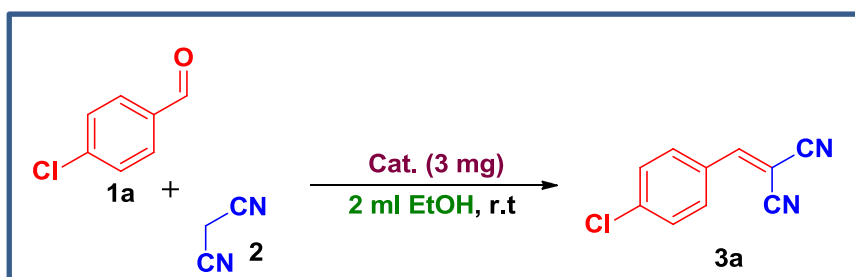


Figure 16. Reaction model: Condensation of 4-chlorobenzaldehyde 1a and malononitrile 2

After proving that the clay after adsorption (Cu-MC) is an excellent heterogeneous catalyst for the synthesis of 3a compound under optimal conditions and to better

confirm that these conditions are valid for Knoevenagel condensation, we have condensed a variety of aromatic aldehydes with malononitrile (Figure17.).

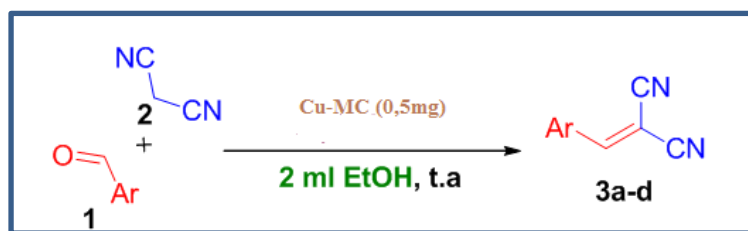


Figure 17. Synthesis of alkenes catalyzed by the Cu-MC

Table 12 shows that 3a-d compounds are produced with good to excellent yields. Apparently, the Knoevenagel condensation not significantly affected by the nature of the substituent linked to aryl group of aldehyde. These results show the effectiveness of our catalytic system. Then we studied one of the most important parameters in green chemistry, which is the reuse catalyst. For this reason, we performed the model reaction under the optimal conditions (0.5mg (Cu-MC), 2 ml EtOH at room temperature). The catalyst removed from the reactive mixture by simple filtration was washed with ethanol and dried in the oven. The recycled catalyst can be used for subsequent reactions without loss of catalytic activity. As

indicated in Table 13, it is clear from the latter that our catalyst could be recycled for five successive cycles without any significant loss of its catalytic power. To finalize our study, we compared the catalytic power of our catalyst with other catalysts reported in the bibliography. Results are grouped in Table 14. These results show that the catalytic capacity of our catalyst (Cu-MC) is greater than those reported in the literature (short reaction time, excellent performance, mild reaction conditions). Therefore, we believe that this simple, rapid and effective method is an improvement over other procedures.

Table 9. Catalytic test on reaction model.

Entry	Catalyst	Time (min) <sup>b</sup>	Rdt (%) <sup>a</sup>
1	Without Catalyst	180	54
2	Clay before adsorption (C <sub>b</sub> )	30	72
3	Clay after adsorption (C <sub>a</sub> )	10	87

<sup>a</sup>Isolated yields; <sup>b</sup>Time reported in min monitored by TLC.

Table 10. Study of solvent effect on reaction model

Entry	Solvent (2ml)	Time (min) <sup>b</sup>	Rdt (%) <sup>a</sup>
1	EtOH	10	87
2	MeOH	10	80
3	H <sub>2</sub> O	20	42
4	CH <sub>3</sub> CN	35	33
4	CH <sub>3</sub> CN	35	33

<sup>a</sup>Isolated yields; <sup>b</sup>Time reported in min monitored by TLC.

Table 11. Mass Effect of Catalyst in reaction model

Entry	C <sub>a</sub> (mg)	Time (min) <sup>b</sup>	Rdts (%) <sup>a</sup>
1	0.5	5	97
2	1	5	94
3	2	7	90
4	3	10	87
5	4	10	82
6	5	10	80

<sup>a</sup>Isolated yields; <sup>b</sup>Time reported in min monitored by TLC.

**Table 12.** Generalization of the Knoevenagel reaction

Product	MC	Time(min)	Rdt (%) <sup>a</sup>	Melting point °C	
				Find	Lit.
<b>3a</b>	<i>p</i> -ClC <sub>6</sub> H <sub>4</sub>	5	97	160-162	158-159 <sup>[14]</sup>
<b>3b</b>	<i>p</i> -MeC <sub>6</sub> H <sub>4</sub>	30	95	118-119	118-119 <sup>[14]</sup>
<b>3c</b>	<i>p</i> -NO <sub>2</sub> C <sub>6</sub> H <sub>4</sub>	5	99	118-119	118-119 <sup>[14]</sup>
<b>3d</b>	C <sub>6</sub> H <sub>5</sub>	60	89	80-81	80-81 <sup>[14]</sup>

<sup>a</sup>Isolated yields; <sup>b</sup>Time reported in min monitored by TLC.**Table 13.** Catalyst recycling study in Knoevenagel 3a condensation.

Product	Number of cycles				
	1	2	3	4	5
<b>3a</b>	97	97	94	94	90

**Table 14.** Comparison of the effectiveness of clay after adsorption (Cu-MC) with other catalysts.

Catalyst	Reaction conditions English	Rdt (%) <sup>a</sup>
<b>CaPO<sub>4</sub>·2H<sub>2</sub>O</b>	0.01g, 3ml EtOH, t.a, 10min	80-96 <sup>[14]</sup>
<b>PMO-IL-NH<sub>2</sub></b>	0.5mol%, Sans solvant, t.a, 90-180min	88-97 <sup>[9]</sup>
<b>Na<sub>2</sub>Ca(HPO<sub>4</sub>)<sub>2</sub></b>	0.006g, 3ml EtOH, t.a, 10-65min	82-99 <sup>[15]</sup>
<b>RhPt@GO NPs</b>	0.07mmol, H <sub>2</sub> O:MeOH,(1,2),t.a, 8-35min	85-90 <sup>[16]</sup>
<b>ZrKP-MePh</b>	2mol%, sans solvant, t.a, 1h	94-96 <sup>[17]</sup>
<b>Cu-MC</b>	<b>0.5 mg, 2 ml EtOH, t.a, 5-60 min</b>	<b>89-99 (Present work)</b>

<sup>a</sup>Isolated yields; <sup>b</sup>Time reported in min monitored by TLC.

## CONCLUSIONS

In this research study, MC has a promising adsorption rate for the elimination of Cu(II) ions. The operative parameters for adsorption were the concentration of copper solution (10 mg/L), sorbent assay (0.5g/100 ml) and temperature (293 K). The elimination of Cu (II) ion depends on the pH and the optimal adsorption was obtained at pH=5.5. For adsorption isotherme, non-linear isotherm method has preferable performances, compared with linear isotherm. The results presented that the non-linear Freundlich isotherm is a more suitable model for describing the adsorption of Cu (II) ions on MC Adsorption kinetics are described by pseudo second-order model.

The second part of this study is the application of Cu-MC as a recyclable heterogeneous catalyst for the condensation of Knoevenagel resulting an excellent yield (87%), an operational simplicity, additional to a low environmental impact and could be used for five cycles without any significant loss of its catalytic power.

## ACKNOWLEDGEMENTS

The authors also gratefully acknowledge the center (CUEATT) of Ibn tofail University, kenitra and center of analysis and characterization (CAD) of Cadi ayyad University, Marrakech, Morocco.

### Competing interests

The authors have declared that no competing interests exist.

## REFERENCES

1. Tizaoui K., Benguella B., Makhoukhi B., 2019. Selective Adsorption of Heavy Metals (Co<sup>2+</sup>, Ni<sup>2+</sup>, and Cr<sup>3+</sup>) from Aqueous Solutions onto Natural Marne Clay. Desalination Water Treat. 142, 252–259.
2. Calagui M.J.C., Senoro D.B., Kan C.C., Salvacion J.W., Futralan C.M., Wan M.W., 2014. Adsorption of Indium (III) Ions from Aqueous Solution Using Chitosan-Coated Bentonite Beads. J Hazard Mater. 277, 120–126.
3. Bouna L., Ait El Fakir A., Abdeljalil B., Draoui K., Villain S., Guinneton F., 2020. Physico-Chemical Characterization of Clays from Assa-Zag for Valorization in

- Cationic Dye Methylene Blue Adsorption. *Mater. Today Proc.* 22, 22-27.
4. Alshameri A., He H., Zhu J., Xi Y., Zhu R., Ma L., Tao Q., 2018. Adsorption of Ammonium by Different Natural Clay Minerals: Characterization, Kinetics and Adsorption Isotherms. *Appl Clay Sci.* 159, 83–93.
  5. Ouaddari H., Beqqour D., Bennazha J., El Amrani I.E., Albizane A., Solhy A., Varma R.S., Natural Moroccan Clays: Comparative Study of Their Application as Recyclable Catalysts in Knoevenagel Condensation. *Sustain Chem Pharm.* 10, 1–8.
  6. Lamberth C., Godineau E., Smejkal T., Trah S., 2012. ChemInform Abstract: A New Knoevenagel-Type Synthesis of Fully Substituted  $\gamma$ -Hydroxybutenolides. *Tetrahedron Lett.* 53, 4117–4120.
  7. Heydari R., Tahamipour B., 2011. Highly Regioselective Synthesis of Dicyano-8a,10,11-Trihydropyrrolo[1,2-a][1,10]Phenanthrolines via a Domino-Knoevenagel-Cyclization. *Chin Chem Lett.* 22(11), 1281–1284.
  8. Tietze L.F., Rackelmann N., 2004. Domino Reactions in the Synthesis of Heterocyclic Natural Products and Analogs. *Pure Appl Chem.* 76(11), 1967–1983.
  9. Vijender M., Kishore P., Satyanarayana B., 2008. Zirconium Tetrachloride-SiO<sub>2</sub> Catalyzed Knoevenagel Condensation: A Simple and Efficient Protocol for the Synthesis of Substituted Electrophilic Alkenes. *Arkivoc.* 13, 122–128.
  10. Alandis N.M., Mekhamer W., Aldayel O., Hefne J.A.A., Alam M., 2019. Adsorptive Applications of Montmorillonite Clay for the Removal of Ag(I) and Cu(II) from Aqueous Medium. *J Chem.* 1-7.
  11. Rosati O., Lanari D., Scavo R., Persia D., Marmottini F., Nocchetti M., Curini M., Piermatti O., 2018. Zirconium Potassium Phosphate Methyl and/or Phenyl Phosphonates as Heterogeneous Catalysts for Knoevenagel Condensation under Solvent Free Conditions. *Microporous Mesoporous Mater.* 268, 251–259.
  12. Çimen O., Koç Ş., Sari A., 2013. Rare earth element (REE) geochemistry and genesis of oil shales around Daghacilair village, Goynuk-Bolu, Turkey. *Oil Shale.* 30(3), 419.
  13. Gionis V., Kacandes G.H., Kastritis I.D., 2006. Chryssikos G.D., On the Structure of Palygorskite by Mid-and near-Infrared Spectroscopy. *Am Mineral.* 91(7), 1125–1133.
  14. Suarez M., Garcia-Romero E., 2006. FTIR Spectroscopic Study of Palygorskite: Influence of the Composition of the Octahedral Sheet. *Appl Clay Sci.* 31 (1–2), 154–163.
  15. Blanco C., González F., Pesquera C., Benito I., Mendioroz S., Pajares J.A., 1989. Differences between One Aluminic Palygorskite and Another Magnesian by Infrared Spectroscopy. *Spectrosc Lett.* 22(6), 659–673.
  16. Yan W., Liu D., Tan D., Yuan P., Chen M., 2012. FTIR Spectroscopy Study of the Structure Changes of Palygorskite under Heating. *Spectrochim. Acta A Mol Biomol Spectrosc.* 97, 1052–1057.
  17. Jiang M., Jin X., Lu X.Q., Chen Z., 2010. Adsorption of Pb (II), Cd (II), Ni (II) and Cu (II) onto Natural Kaolinite Clay. *Desalination.* 252 (1–3), 33–39.
  18. Essebaai H., Ismi I., Lebki A., Marzak S., 2019. Kinetic and Thermodynamic Study of Adsorption of Copper (II) Ion on Moroccan Clay. *Mediterr J Chem.* 9 (2), 102–115.
  19. Van Tran T., Nguyen D.T.C., Le H.T., Tu T.T., Le N.D., Lim K.T., Bach L.G., Nguyen T.D., 2019. MIL-53 (Fe)-Directed Synthesis of Hierarchically Mesoporous Carbon and Its Utilization for Ciprofloxacin Antibiotic Remediation. *J Environ Chem Eng.* 7(1), 102881.
  20. Nartowska E., 2019. The Effects of Potentially Toxic Metals (Copper and Zinc) on Selected Physical and Physico-Chemical Properties of Bentonites. *Heliyon.* 5(10), e02563.
  21. Ndzana G.M., Huang L., Zhang Z., Zhu J., Liu F., Bhattacharyya R., 2019. The Transformation of Clay Minerals in the Particle Size Fractions of Two Soils from Different Latitude in China. *Catena.* 175, 317–328.
  22. Lagergren S., 1899. Zur Theorie der sogenannten Adsorption gelöster Stoffe. *Physik Ch.* 32, 174–75.
  23. Ho Y.S., McKay G., 1999. Pseudo-Second Order Model for Sorption Processes. *Process Biochem.* 34(5), 451–465.
  24. Fu J., Xin Q., Wu X., Chen Z., Yan Y., Liu S., Wang M., Xu Q., 2016. Selective Adsorption and Separation of Organic Dyes from Aqueous Solution on Polydopamine Microspheres. *J Colloid Interface Sci.* 461, 292–304.
  25. Mahmoodi N.M., 2015. Surface Modification of Magnetic Nanoparticle and Dye Removal from Ternary Systems. *J Ind Eng Chem.* 27, 251–259.

26. Bentahar S., Dbik A., El Khomri M., El Messaoudi N., Lacherai A., 2017. Adsorption of Methylene Blue, Crystal Violet and Congo Red from Binary and Ternary Systems with Natural Clay: Kinetic, Isotherm, and Thermodynamic. *J Environ Chem Eng.* 5(6), 5921–5932.
27. Weber W.J., Morris J.C., 1963. Kinetics of Adsorption on Carbon from Solution. *J Sanit Eng Div.* 89(2), 31–60.
28. Chowdhury S., Misra R., Kushwaha P., Das P., 2011. Optimum Sorption Isotherm by Linear and Nonlinear Methods for Safranin onto Alkali-Treated Rice Husk. *Bioremediation J.* 15(2), 77–89.
29. Benderdouche N., Bestani B., Hamzaoui M., 2018. The Use of Linear and Nonlinear Methods for Adsorption Isotherm Optimization of Basic Green 4-Dye onto Sawdust-Based Activated Carbon. *J Mater Env Sci.* 9, 1110–1118.
30. Jeppu G.P., Clement T.P., 2012. A Modified Langmuir-Freundlich Isotherm Model for Simulating PH-Dependent Adsorption Effects. *J Contam Hydrol.* 129, 46–53.
31. Chen X., 2015. Modeling of Experimental Adsorption Isotherm Data. *Information.* 6(1), 14–22.
32. Kapoor A., Yang R.T., 1989 Correlation of Equilibrium Adsorption Data of Condensable Vapours on Porous Adsorbents. *Gas Sep. Purif.* 3(4), 187–192.
33. Kausar A., Naeem K., Hussain T., Bhatti H.N., Jubeen F., Nazir A., Iqbal M., 2019. Preparation and Characterization of Chitosan/Clay Composite for Direct Rose FRN Dye Removal from Aqueous Media: Comparison of Linear and Non-Linear Regression Methods. *J Mater Res Technol.* 8(1), 1161–1174.
34. Amrhar O., Nassali H., Elyoubi M.S., 2015. Application of Nonlinear Regression Analysis to Select the Optimum Absorption Isotherm for Methylene Blue Adsorption onto Natural Illitic Clay. *Bull Société R Sci Liège.* 84, 116–130.
35. Vasanth Kumar K., Sivanesan S., 2005. Comparison of linear and non-linear method in estimating the sorption isotherm parameters for safranin onto activated carbon. *Journal of Hazardous Materials B123,* 288–292.